The apparent diffusion coefficient can serve as a predictor of survival in patients with gliomas

Xue Jiang[1,3†], Xu-Ni Xu[2,3†], Xiao-Ye Yuan[3], Hao-Ran Jiang[3], Meng-Jing Zhao[4], Yu-Xia Duan[4*] and Gang Li[3*]

Abstract

Background and purpose Magnetic resonance imaging is indispensable for the preoperative diagnosis of glioma. This study aimed to investigate the role of the apparent diffusion coefficient values as predictors of survival in patients with gliomas.

Methods and materials A retrospective analysis was conducted on 101 patients with gliomas who underwent surgery between 2015 and 2020. Diffusion-weighted MRI was performed before the surgery. The regions of interest were categorized into parenchymal area, non-enhancing peritumoral area, and necrotic or cystic area. All the patients were divided into three subgroups: the parenchyma group, the non-enhancing peritumoral signal abnormality group, and the necrosis or cyst group. Univariate and multivariate analyses were performed using COX regression.

Results In the parenchymal group, Ki67, P53, IDH, and the high or low ADC values were identified as independent prognosticators for disease-free survival, while Ki67, IDH, and the high or low ADC values for overall survival. In the non-enhancing peritumoral signal abnormality group, Ki67, P53, IDH, and the $ADC_{parenchymal\ area}/ADC_{non-enhancing\ peritumoral\ area}$ ratio were identified as independent prognostic factors for disease-free survival, while Ki67, IDH, and the $ADC_{parenchymal\ area}/ADC_{non-enhancing\ peritumoral\ area}$ ratio for overall survival. In the necrosis or cyst group, Ki67 was significantly associated with disease-free survival, while Ki67 and the ADC value of the necrotic or cystic area for overall survival.

Conclusions The ADC values, including the ADC value in the parenchymal area, the $ADC_{parenchymal\ area}/ADC_{non-enhancing\ peritumoral\ area}$ ratio, and the ADC value in the necrotic or cystic area, can serve as an efficient and potential index for predicting the survival of patients with glioma.

Keywords Apparent diffusion coefficient, Gliomas, Disease-free survival, Overall survival

†Xue Jiang and Xu-Ni Xu contributed equally to this work.

*Correspondence:
Yu-Xia Duan
doughter1@163.com
Gang Li
andrewlee0923@wzhospital.cn

¹Department of Pathology, Jinhua Municipal Central Hospital, Affiliated Jinhua Hospital, Zhejiang University School of Medicine, Jinhua, Zhejiang 321000, China
²Department of Radiology, Shaoxing Central Hospital, The Central Hospital of Shaoxing University, Shaoxing, Zhejiang 312030, China
³Department of Radiation Oncology, The First Affiliated Hospital of Wenzhou Medical University, Wenzhou, Zhejiang 325000, China
⁴Department of Radiology, The First Affiliated Hospital of Wenzhou Medical University, Wenzhou, Zhejiang 325000, China

Jiang *et al. Radiation Oncology*   (2024) 19:149

Page 2 of 11

Introduction

Gliomas are the most common primary intracranial tumors, which account for about 80% of brain malignancies [1], with a global incidence rate of 5 to 6 cases per 100,000 people each year [2]. The 5-year survival rate is only 5% for glioblastoma [1]. Gliomas of the central nervous system were classified into low-grade (grades I, II) and high-grade (grades III, IV) by the World Health Organization (WHO) [3]. The main treatments for gliomas include surgical resection, adjuvant chemotherapy, and radiotherapy [4, 5]. Despite the comprehensive treatment options available for glioma patients, the overall prognosis remains poor. Currently, there is still a lack of effective methods to predict the survival outcomes for individuals diagnosed with glioma.

Magnetic resonance imaging (MRI) is a commonly used non-invasive diagnostic method in the preoperative diagnosis of gliomas [6]. Due to DNA-sequencing is either costly and difficult to achieve in the process of pathological diagnosis, by evaluating the enhancement, necrosis, edema, angiogenesis and other aspects of the tumor on MRI, the preliminary diagnosis of the tumor classification and grade can be made, which is important for the diagnosis and treatment of patients in some special cases [7]. Diffusion-weighted imaging (DWI), a specialized functional MRI technique, possesses sensitivity to the motion of water molecules within living tissues [8]. The apparent diffusion coefficient (ADC) is derived from DWI and displayed as a parametric map. The value of ADC is calculated based on the fluidity of water molecules and the density of cells, which has the potential to noninvasively assess the overall hypoxic status of tumors [9]. It is an important indicator for evaluating treatment efficacy and tumor progression or recurrence [10, 11]. Higher ADC values indicate greater fluidity and lower cell density [12]. Previous reports have indicated a relationship between ADC values in the parenchymal area of gliomas and patient's survival [13, 14]. Due to the obstruction of the flow of water molecules, the ADC value of highly cellular tissue is lower. The lower the ADC value, the worse the patient's prognosis. While in high-grade gliomas, the presence of edema and necrosis has been found to correlate with survival [15, 16]. Glioblastoma patients with less necrosis have longer survival times, and peritumoral edema is associated with poor prognosis [15]. The survival rate of glioblastoma patients with necrosis is lower than that of patients without necrosis [16]. Since peritumoral edema contains tumor cells, the P/N ratio ($ADC_{parenchymal\ area}/ADC_{non-enhancing\ peritumoral\ area}$) was included in this study. To the current knowledge, no prior research has been explored to investigate the connection between survival and the P/N ratio. Therefore, it is necessary to measure the ADC value in different regions to predict the survival of patients.

In this study, the ADC value in the parenchymal area, the P/N ratio and the ADC value in the necrotic or cystic (N/C) area were calculated to explore the relationship with disease-free survival (DFS) and overall survival (OS).

Methods

Patient population

A retrospective analysis was conducted on a total of 101 patients with gliomas who underwent surgical resection followed by radiotherapy in combination with temozolomide at the First Affiliated Hospital of Wenzhou Medical University from November 2015 to October 2020. The inclusion criteria for this study were as follows: (1) histopathologically confirmed diagnosis of gliomas based on the World Health Organization criteria by at least one expert pathologist; (2) availability of MRI examination with DWI sequence prior to the surgery; (3) no previous antitumor treatment prior to the surgery; (4) administration of radiotherapy and chemotherapy after the surgery. Patients who had conditions such as severe cardio-cerebrovascular disease, other malignant tumors, and a large number of extracranial tumors that could potentially decrease their chances of survival were not included in the study. These exclusion criteria aimed to ensure that the focus of the research was on patients with the highest likelihood of achieving positive outcomes. The scientific investigation took place at the First Affiliated Hospital of Wenzhou Medical University and received approval from the Institutional Review Board. The need for written informed consent was exempted.

Magnetic resonance imaging

All the 101 patients participated in the study and underwent a series of brain scans using a 3.0 Tesla MRI scanner (Philips Achieva, Philips Medical System) equipped with an 8-channel receive-only head coil. The MRI scans included T1-weighted imaging (T1WI), T2-weighted imaging (T2WI), contrast-enhanced T1WI, fluid-attenuated inversion recovery (FLAIR), and diffusion-weighted imaging (DWI) before the surgery. The DWI scans were obtained in the transverse plane using a spin echo-echo planar imaging (SE-EPI) sequence, which had the following parameters: echo time/repetition time (TE/TR)=109/3234 ms, field of view=230×230 mm^2, matrix=128×128, slice thickness=5.0 mm, and b-values=0, 1000 s/mm^2. The mean ADC value of the region of interest (ROI) was calculated from the DWI scans obtained at b-values of 0 and 1000 s/mm^2 using the MicroDicom DICOM Viewer software 2022.3 (Build 4004).

Imaging analysis and regions of interest (ROI)

The ROIs were divided into three areas by using three different colored lines: parenchymal area, non-enhancing

peritumoral area, and N/C area (Fig. 1). All slices containing these areas were drawn in transverse section, and at each slice, the largest area was plotted along the lesion area. In this study, DWI images with a b-value of 1000 s/mm^2 were manually used to place the ROIs. Then, the DWI images with a b-value of 0 s/mm^2 were duplicated by using these ROIs. According to the ADC value calculation formula, the ADC values of different areas on each slice were calculated firstly, and then the average ADC values of different regions were calculated according to these ADC values. To ensure accuracy and impartiality, an experienced radiologist analyzed the pre-surgery magnetic resonance (MR) images and DW images. This radiologist was blinded to the pathology reports and clinical patient data, which reduced the possibility of bias. In case of any uncertainties or disagreements, another senior radiologist was consulted for resolution.

Treatment

All the patients enrolled underwent gross total resection. However, due to the invasive nature of high-grade gliomas, completely removing the tumor pathologically can be challenging. To achieve the maximum safe resection of high-grade gliomas, new surgery-assisted techniques such as neural image navigation and intraoperative neuroelectrophysiological monitoring was applied. After the surgery, all the patients received radiotherapy (54 ~ 60 Gy for 5 ~ 6 weeks) concurrent with simultaneous TMZ

chemotherapy. Six cycles of adjuvant chemotherapy were administered after concurrent chemoradiotherapy.

Follow-up

OS and DFS were the primary endpoints in this study. The assessment of OS involved determining the length of time between surgical intervention and either the occurrence of death or the end of the study period. Similarly, DFS was calculated by evaluating the time between the surgical procedure and the initial occurrence of recurrence, death, or the conclusion of the study period, whichever occurred first.

Statistical analysis

The patients were divided into three subgroups: the parenchymal group, the non-enhancing peritumoral signal abnormality (NEPSA) group, and the N/C group. For the parenchymal group, the ADC value of the parenchymal area was analyzed using the X-tile software to classify it into high ADC value and low ADC value. Univariate and multivariate Cox regression analysis was conducted to examine the factors influencing DFS and OS, and the Kaplan-Meier method was used to visualize the results. In the NEPSA group, the P/N ratio was used for analysis. Furthermore, the COX proportional hazard regression model was employed to investigate the relationship between DFS, OS, and the relevant factors. In the N/C group, the association between the ADC value of the N/C
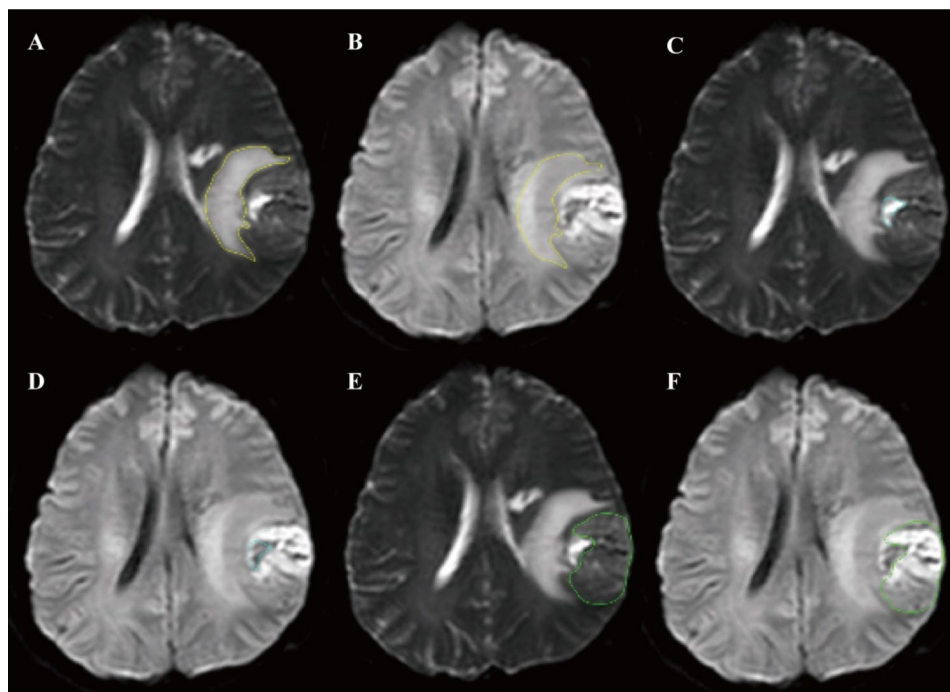

Fig. 1 Tumor segmentation in DWI MRI. (**A**) non-enhancing peritumoral area in DWI with the b-value of 0 s/mm^2. (**B**) non-enhancing peritumoral area in DWI with the b-value of 1000 s/mm^2. (**C**) Necrotic area in DWI with the b-value of 0 s/mm^2. (**D**) Necrotic area in DWI with the b-value of 1000 s/mm^2. (**E**) Parenchymal area in DWI with the b-value of 0 s/mm^2. (**F**) Parenchymal area in DWI with the b-value of 1000 s/mm^2

Jiang *et al. Radiation Oncology*   (2024) 19:149

Page 4 of 11

area and DFS or OS was examined. A statistically significant difference was defined as a p-value less than 0.05. All statistical analyses in this article were performed using commercially available statistical software (version 4.2.2, R Statistics Software, Inc.).

Results

Patient characteristics and survival

The characteristics of 101 patients with gliomas are summarized in Table 1. The results of mean ADC measurement were 1.186 (ranging from 0.679 to 1.770) ($\times 10^{-3}$ mm^2/s) in parenchymal area with 101 patients; 1.306

Table 1 Patient characteristics

Variables	Values	Range or percent
Total no. of patients	101	
Age, years		
≤ 52	55	54.5%
> 52	46	45.5%
Gender		
Male	53	52.5%
Female	48	47.5%
Glioblastoma		
Yes	67	66.3%
No	34	33.7%
Location		
Occipital lobe	5	5.0%
Parietal lobe	22	21.8%
Temporal lobe	31	30.7%
Frontal lobe	33	32.7%
Other	10	9.9%
Grade		
Low	18	17.8%
High	83	82.2%
Ki67		
≤ 10%	29	28.7%
> 10%	72	71.3%
P53		
Positive	70	69.3%
Negative	31	30.7%
MGMT		
Positive	61	60.4%
Negative	40	39.6%
IDH		
Positive	32	31.7%
Negative	69	68.3%
Tumor maximum diameter		
≤ 38 mm	32	31.7%
> 38 mm	69	68.3%
NEPSA		
Yes	70	69.3%
No	31	30.7%
Necrosis or cyst		
Yes	75	74.3%
No	26	25.7%

(ranging from 0.816 to 1.552) ($\times 10^{-3}$ mm^2/s) in non-enhancing peritumoral area with 70 patients; 1.793 (ranging from 1.065 to 2.483) ($\times 10^{-3}$ mm^2/s) in N/C area with 75 patients. The median follow-up time for the patients was 51.8 months, ranging from 30.23 to 87.03 months. Out of the 101 patients, 62 experienced a relapse, with a median disease-free survival time of 18.8 months (ranging from 0.63 to 57.50 months). Among them, 50 patients with glioblastoma relapsed and 12 patients with non-glioblastoma relapsed. Additionally, 70 patients died, with a median survival time of 24.7 months (ranging from 1.73 to 68.57 months). Among them, 58 patients with glioblastoma died and 12 patients with non-glioblastoma died.

The subgroup of the patients who had parenchymal area

All the patients included in the study exhibited parenchymal area. The cut-off value for ADC in the parenchymal area was determined using X-tile software (V.3.6.1). An ADC value more than 1.123×10^{-3} mm^2/s was classified as high, while the remaining values were classified as low.

A wide range of factors were evaluated using Kaplan-Meier curves and cox regression analysis to determine prognostic factors for postoperative survival. Univariate and multivariate cox regression analysis indicated that Ki67, P53, IDH, and high or low ADC value were independent prognostic factors for DFS (Fig. 2A-D; Table 2).

The same approach was used to identify OS-associated features, such as age, presence of glioblastoma, grade, Ki67, P53, IDH, NEPSA, status of N/C, and high or low ADC value per univariate cox regression analysis. Multivariate Cox regression analysis revealed that Ki67, IDH, and high or low ADC value were independent prognostic factors for postoperative OS (Fig. 2E-G; Table 3).

The subgroup of the patients who had non-enhancing peritumoral area

A total of 70 patients with non-enhancing peritumoral area were included in the study. Univariate COX regression analysis revealed that the ADC value of the non-enhancing peritumoral area did not show any statistically significant association. However, the ADC value of the parenchymal area showed a statistically significant association with DFS and OS when analyzed. Therefore, the P/N ratio was incorporated in the subsequent analysis.

The study analyzed various factors such as age, gender, presence of glioblastoma, location, grade, Ki67, P53, MGMT, IDH, tumor maximum diameter, status of N/C, and the P/N ratio to determine their association with DFS. To assess these characteristics, univariate and multivariate cox regression analyses were performed. The results showed that Ki67 (*P*=0.013), P53 (*P*=0.043), IDH (*P*=0.042), and the P/N ratio (*P*=0.030) were independent prognostic factors for DFS. Similarly, the study identified that Ki67 (*P*=0.015), IDH (*P*=0.009), and the P/N
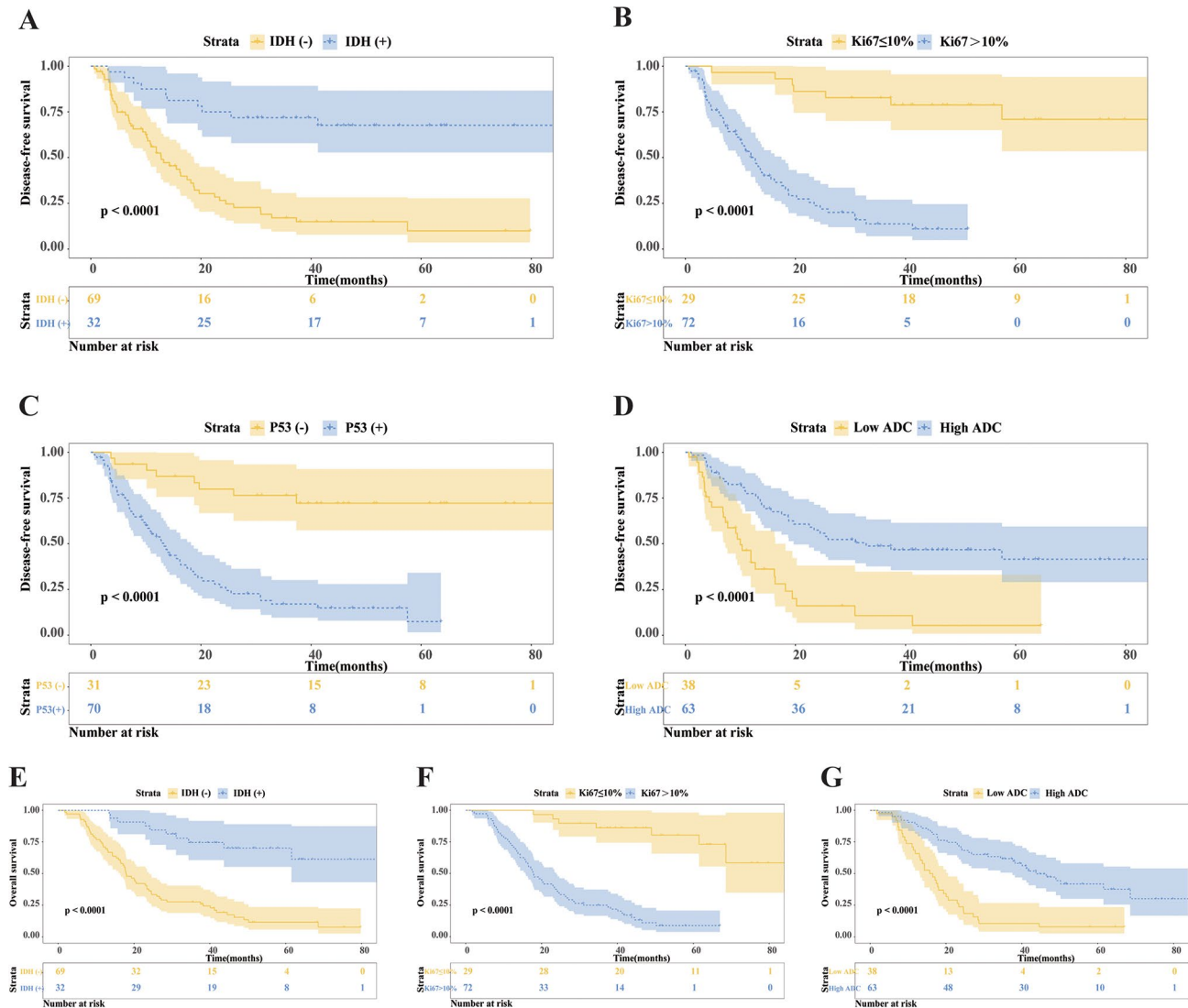
Fig. 2 Disease-free survival (DFS) and Overall survival (OS) analysis. (**A**) Kaplan–Meier DFS curves of IDH. (**B**) Kaplan–Meier DFS curves of Ki67. (**C**) Kaplan–Meier DFS curves of P53. (**D**) Kaplan–Meier DFS curves of high or low ADC value. (**E**) Kaplan–Meier OS curves of IDH. (**F**) Kaplan–Meier OS curves of Ki67. (**G**) Kaplan–Meier OS curves of high or low ADC value

ratio ($P=0.047$) were independent prognostic factors for OS using the same method.

Ki67, P53, IDH, and the P/N ratio were utilized to develop a nomogram model for predicting DFS and the DFS rates at 1, 2, and 3 years (Fig. 3A). Similarly, Ki67, IDH, and the P/N ratio were employed to construct a nomogram for predicting postoperative OS and the OS rates at 1, 2, and 3 years (Fig. 3D).

The study conducted a comprehensive evaluation of nomograms for discrimination, calibration, and clinical utility. This evaluation involved the use of various measurements such as C-index, receiver operating characteristic (ROC), calibration plot, and decision curve analysis (DCA). Specifically, the nomogram for DFS demonstrated a C-index of 0.734 (95% confidence interval: 0.664–0.817). Additionally, the area under the curve

(AUC) for the predictions of DFS at 1-, 2-, and 3-year intervals were found to be 0.823, 0.839, and 0.875, respectively (Fig. 3B). Similarly, the nomogram for postoperative OS exhibited a C-index of 0.760 (95% confidence interval: 0.692–0.821). The AUCs for the predictions of OS at 1-, 2-, and 3-year intervals were determined to be 0.811, 0.864, and 0.827, respectively (Fig. 3E).

Calibration plots were created to compare nomogram-predicted outcomes with actual outcomes for 1-year, 2-year, and 3-year DFS/OS rates, demonstrating the high quality of the nomogram (Fig. 3C and F). The calibration curves graphically represented the predicted DFS or OS incidence on the x-axis and the observed actual DFS or OS incidence on the y-axis, ranging from 0 to 1, which represented the event incidence. The reference line, shown as a grey diagonal line, represented the predicted

Table 2 Univariable and multivariable cox regression analysis for DFS

Variables	Univariate analysis		Multivariate analysis	
	HR (95% CI)	*P* value	HR (95% CI)	*P* value
Age, years				
≤52	1			
>52	2.722 (1.774–4.177)	<0.001*	1.260 (0.799–1.986)	0.404
Gender			Not selected	
Male	1.313 (0.862–2.001)	0.287		
Female	1			
Glioblastoma				
Yes	4.354 (2.538–7.470)	<0.001*	0.700 (0.326–1.504)	0.443
No	1			
Location			Not selected	
Occipital lobe	0.328 (0.098–1.171)	0.151		
Parietal lobe	1			
Temporal lobe	0.736 (0.417–1.297)	0.373		
Frontal lobe	0.660 (0.377–1.157)	0.224		
Other	1.104 (0.523–2.330)	0.828		
Grade				
Low	1			
High	8.733 (3.282–23.238)	<0.001*	1.294 (0.376–4.447)	0.731
Ki67				
≤10%	1			
>10%	9.432 (4.580-19.423)	<0.001*	3.043 (1.349–6.866)	0.024*
P53				
Positive	6.146 (3.260-11.589)	<0.001*	2.416 (1.170–4.986)	0.045*
Negative	1			
MGMT			Not selected	
Positive	0.853 (0.558–1.302)	0.536		
Negative	1			
IDH				
Positive	0.199 (0.112–0.356)	<0.001*	0.342 (0.180–0.647)	0.006*
Negative	1			
Tumor maximum diameter			Not selected	
≤38 mm	1			
>38 mm	1.302 (0.814–2.082)	0.353		
NEPSA				
Yes	2.576 (1.537–4.316)	0.003*	2.052 (1.055–3.990)	0.076
No	1			
Necrosis or cyst				
Yes	2.996 (1.650–5.439)	0.002*	1.792 (0.967–3.321)	0.120
No	1			
ADC $_{parenchymal\ area}$				
Low	1			
High	0.314 (0.203–0.486)	<0.001*	0.401 (0.242–0.664)	0.003*

value equaling the actual value. The curve fitting line, which closely followed the grey diagonal line, indicated higher accuracy, and the colored area on both sides represented the 95% confidence interval.

The decision curve analysis demonstrated the value of the two models. The net benefit of 3-year DFS was consistently higher than that at other time points across a wide range of reasonable threshold probabilities, as illustrated in Fig. 3G-L.

The subgroup of the patients who had N/C area

A total of 75 patients with N/C areas were included in the study. Various factors such as age, gender, presence of glioblastoma, location, grade, Ki67, P53, MGMT, IDH, tumor maximum diameter, NEPSA, and the ADC value of N/C area were analyzed using univariate cox regression analysis to determine their association with DFS. The results of cox regression analyses revealed that only

Table 3 Univariable and multivariable cox regression analysis for OS

Variables	Univariate analysis		Multivariate analysis	
	HR (95% CI)	*P* value	HR (95% CI)	*P* value
Age, years				
≤52	1			
>52	3.078 (2.049–4.625)	< 0.001*	1.273 (0.821–1.974)	0.364
Gender			Not selected	
Male	1.591 (1.064–2.378)	0.092		
Female	1			
Glioblastoma				
Yes	4.568 (2.698–7.733)	< 0.001*	1.041 (0.699–2.807)	0.425
No	1			
Location			Not selected	
Occipital lobe	0.337 (0.098–1.161)	0.148		
Parietal lobe	1			
Temporal lobe	1.099 (0.653–1.849)	0.766		
Frontal lobe	0.607 (0.347–1.063)	0.143		
Other	1.198 (0.590–2.430)	0.675		
Grade				
Low	1			
High	8.360 (3.155–22.151)	< 0.001*	0.819 (0.229–2.932)	0.797
Ki67				
≤10%	1			
>10%	10.179 (4.935–20.996)	< 0.001*	3.881 (1.631–9.239)	0.010*
P53				
Positive	4.783 (2.700-8.473)	< 0.001*	1.270 (0.650–2.483)	0.558
Negative	1			
MGMT			Not selected	
Positive	1.028 (0.686–1.541)	0.910		
Negative	1			
IDH				
Positive	0.190 (0.108–0.335)	< 0.001*	0.321 (0.171–0.602)	0.003*
Negative	1			
Tumor maximum diameter			Not selected	
≤38 mm	1			
>38 mm	1.364 (0.876–2.123)	0.248		
NEPSA				
Yes	1.819 (1.157–2.858)	0.030*	1.148 (0.661–1.992)	0.682
No	1			
Necrosis or cyst				
Yes	2.618 (1.521–4.506)	0.004*	1.619 (0.920–2.850)	0.161
No	1			
ADC $_{parenchymal\ area}$				
Low	1			
High	0.291 (0.193–0.438)	< 0.001*	0.383 (0.239–0.614)	< 0.001*

Ki67 ($P=0.004$) was an independent prognostic factor for DFS, while the ADC value of the N/C area was not.

The same method was applied to assess Ki67 ($P=0.007$) and the ADC value of N/C area ($P=0.047$) as independent prognostic factors of OS.

Discussion

MRI is an essential noninvasive imaging method for diagnosing gliomas. Numerous studies have shown that advanced MRI sequences, such as DWI, play a crucial role in tumor grading, predicting therapeutic effectiveness, assessing disease progression, and predicting survival time in glioma patients [17–23]. DWI measures the diffusion of protons in water molecules, allowing the evaluation of cell density and cell membrane integrity
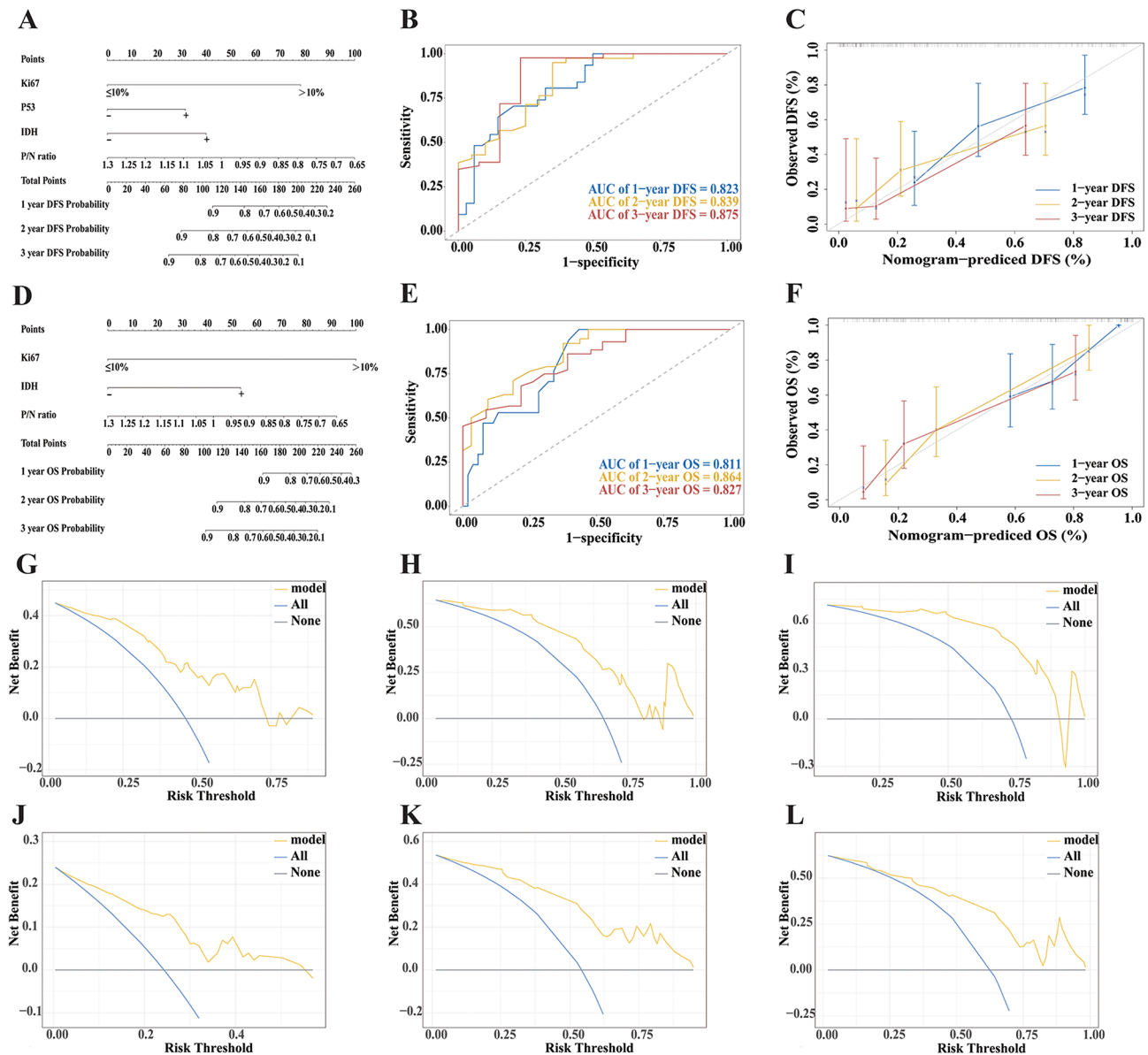
Fig. 3 Construction of the model, time-dependent ROC curves, calibration plots of the nomogram, and decision curve analysis. (**A**) Nomogram for predicting the 1-, 2- and 3-year DFS. (**B**) Time-dependent ROC curves for predicting 1-, 2- and 3-year DFS. (**C**) Calibration curves of the model for predicting DFS at the 1-year, 2-year, and 3-year time points. (**D**) Nomogram for predicting the 1-, 2- and 3-year OS. (**E**) Time-dependent ROC curves for predicting 1-, 2- and 3-year OS. (**F**) Calibration curves of the model for OS at the 1-year, 2-year, and 3-year time points. (**G**) Decision curve analysis of 1-year DFS. (**H**) Decision curve analysis of 2-year DFS. (**I**) Decision curve analysis of 3-year DFS. (**J**) Decision curve analysis of 1-year OS. (**K**) Decision curve analysis of 2-year OS. (**L**) Decision curve analysis of 3-year OS

[24]. The measurement of the ADC of water in vivo is not feasible using MRI directly due to its complex mechanisms. Instead, it is determined indirectly from the ADC acquired via DWI [25]. A negative relationship exists between the value of ADC and cell density. An elevation in ADC indicates a rise in the mobility of water molecules, suggesting either a disruption in the integrity of the membrane or a higher proportion of extracellular fluid caused by a reduction in cell size or count. Conversely, a decline in ADC signifies a decrease in extracellular water

molecules or an expansion in cell size or count [12]. Consequently, the nucleus-to-cytoplasm ratio of the tumor type tends to increase with tumor grade, while the ADC value tends to decrease [26].

In the study by Murakami et al., it was found that high-grade astrocytes with low ADC values generally have a poor prognosis [13]. Saksena et al. also demonstrated that low ADCs in glioblastomas were associated with a worse 6-month progression-free survival rate [27]. In our study, we observed that patients with high ADC values

had longer DFS and OS, which is consistent with other related studies. However, Brasil Caseiras et al. reported that low-grade gliomas had no effect on prognosis in relation to ADC values [28]. This difference can be attributed to the fact that low-grade gliomas generally have longer survival times compared to high-grade gliomas. Additionally, ADC values have also been shown to be a helpful marker for assessing therapy responses in other cancers, such as thymoma, solitary large hepatocellular carcinoma, and gastric cancer [29–31].

Peritumoral edema, which refers to the abnormal accumulation of water in the brain parenchyma, is often observed in patients with gliomas [32]. Previous studies have shown that edema has prognostic significance in multivariable analysis [15]. However, Ramnarayan et al. demonstrated that multivariate analysis did not identify peritumoral edema as an independent predictive factor [33]. In our study, while NEPSA showed prognostic significance in univariate analysis, it did not retain its significance in multivariable analysis. The heterogeneity in patients' clinical characteristics and imaging techniques used among different studies may contribute to these varying results. In glioblastoma cadaver specimens, Burger et al. discovered tumor cell infiltration in the peritumoral edema region [34]. Therefore, we included the P/N ratio in our study, which represents the ratio of tumor cells in the parenchymal area to those in the non-enhancing peritumoral area. To the best of our knowing, there have been no prior studies on the application of this ratio for analysis. Our study revealed that this ratio was a standalone predictive factor in the survival analysis of patients with glioma, covering both DFS and OS. The smaller the ratio, the shorter the survival or recurrence time of the patients, as there is a negative correlation between ADC value and cell density.

It is believed that necrotic areas, which are commonly seen in gliomas on imaging, indicate rapid expansion and malignant behavior. However, the relationship between tumor necrosis and patient survival in gliomas remains controversial. A study involving 416 patients found that the extent of tumor necrosis observed on MR imaging is an independent prognostic characteristic for glioma patients [16]. Another study by David A. Gutman et al. revealed that the percentage of necrosis did not show a substantial correlation with overall survival [35]. The exact mechanism of cyst formation is still not fully understood, and further research is needed. In our study, we found that necrosis or cysts were not independent prognostic factors for survival in all glioma patients. However, in a subgroup analysis of patients with N/C areas, the ADC value of these areas was found to be an independent prognostic variable for OS, but not DFS. This finding may be attributed to the limited number of patients included in our study.

Vascular endothelial growth factor (VEGF) expression is increased in gliomas due to necrosis and hypoxia, which encourages angiogenesis. This process further increases necrosis and enhances resistance to radiotherapy [36]. On the other hand, radiotherapy eliminates tumor cells by generating reactive oxygen species (ROS) in the tumor tissue, which damage the DNA of tumor cells. However, ROS can also activate hypoxia-inducible factors, resulting in an elevation of VEGF levels. This increase in VEGF contributes to angiogenesis and improves the survival rate of tumor cells. Therefore, in the treatment of gliomas, combining radiotherapy with antivascular drugs such as bevacizumab can be considered to reduce the resistance of tumor cells to radiotherapy. Ki67 and IDH were found to be independent prognostic elements for survival, which is consistent with previous studies [37, 38]. In our study, P53 predicted a good prognosis for DFS, but not for OS. However, a recent study indicated a significant difference in the OS period between high expression P53 and low expression P53 [39].

There are several limitations to the current study. Firstly, the number of patients included in the study was small, and therefore, more extensive research is required. Secondly, our study was conducted in a single center, indicating the need for multicenter research. Thirdly, our models lack internal and external verification, which may impact the accuracy and reliability of the study. Fourthly, it is a retrospective study and some missing information may affect the results of the research, thus prospective research needs to be carried out. Additionally, by dividing the lesions into three areas and analyzing them separately, patients may have different prognostic outcomes. Therefore, a larger sample quantity is needed for a consolidated analysis.

Conclusions

The ADC value including the ADC value in parenchymal area, the P/N ratio and the ADC value in N/C area is an efficient and practical potential index to predict the survival of patients with gliomas when compared to the conventional imaging evaluation methods. However, due to the heterogeneity of tumors, relying on ADC values alone can lead to misinterpretations of tumor behavior. Therefore, ADC values are often used in conjunction with other imaging features and clinical information to provide a more comprehensive tumor assessment.

Abbreviations

WHO	World Health Organization
MRI	Magnetic resonance imaging
DWI	Diffusion-weighted imaging
ADC	Apparent diffusion coefficient
P/N ratio	$ADC_{parenchymal\ area}/ADC_{non-enhancing\ peritumoral\ area}$
N/C	Necrotic or cystic
DFS	Disease-free survival

OS	Overall survival
T1WI	T1-weighted imaging
T2WI	T2-weighted imaging
FLAIR	Fluid-attenuated inversion recovery
SE-EPI	Spin echo-echo planar imaging
TE/TR	Echo time/repetition time
ROIs	Regions of interest
MR	Magnetic resonance
NEPSA	Non-enhancing peritumoral signal abnormality
ROC	Receiver operating characteristic
DCA	Decision curve analysis
AUC	Area under the curve
VEGF	Vascular endothelial growth factor
ROS	Reactive oxygen species

Data availability
No datasets were generated or analysed during the current study.

Declarations

Ethics approval and consent to participate
Not applicable.

Consent for publication
Not applicable.

Competing interests
The authors declare no competing interests.

References
1. Ostrom QT, Bauchet L, Davis FG, Deltour I, Fisher JL, Langer CE, Pekmezci M, et al. The epidemiology of glioma in adults: a state of the science review. Neuro Oncol. 2014;16:896–913.
2. McNeill KA. Epidemiology of brain tumors. Neurol Clin. 2016;34:981–98.
3. Lou J, Hao Y, Lin K, Lyu Y, Chen M, Wang H, et al. Circular RNA CDR1as disrupts the p53/MDM2 complex to inhibit Gliomagenesis. Mol Cancer. 2020;19:138.
4. Nageswara Rao AA, Packer RJ. Advances in the management of low-grade gliomas. Curr Oncol Rep. 2014;16:398.
5. Vern-Gross TZ, Schreiber JE, Broniscer A, Wu S, Xiong X, Merchant TE. Prospective evaluation of local control and late effects of conformal radiation therapy in children, adolescents, and young adults with high-grade glioma. Neuro Oncol. 2014;16:1652–60.
6. Wu CX, Lin GS, Lin ZX, Zhang JD, Liu SY, Zhou CF. Peritumoral edema shown by MRI predicts poor clinical outcome in glioblastoma. World J Surg Oncol. 2015;13:97.
7. Pons-Escoda A, Majos C, Smits M, Oleaga L. Presurgical diagnosis of diffuse gliomas in adults: Post-WHO 2021 practical perspectives from radiologists in neuro-oncology units. Radiologia (Engl Ed). 2024;66:260–77.
8. Gadda D, Mazzoni LN, Pasquini L, Busoni S, Simonelli P, Giordano GP. Relationship between Apparent Diffusion coefficients and MR Spectroscopy findings in High-Grade Gliomas. J Neuroimaging. 2017;27:128–34.
9. Shu C, Wang J. The relationship between MRI quantitative parameters and the expression of hypoxia inducible factor-1 alpha in cerebral astrocytoma. Clin Neurol Neurosurg. 2017;153:14–9.
10. Kim S, Loevner L, Quon H, Sherman E, Weinstein G, Kilger A, et al. Diffusion-weighted magnetic resonance imaging for predicting and detecting early response to chemoradiation therapy of squamous cell carcinomas of the head and neck. Clin Cancer Res. 2009;15:986–94.
11. Dirix P, Vandecaveye V, De Keyzer F, Stroobants S, Hermans R, Nuyts S. Dose painting in radiotherapy for head and neck squamous cell carcinoma: value of repeated functional imaging with (18)F-FDG PET, (18)F-fluoromisonidazole PET, diffusion-weighted MRI, and dynamic contrast-enhanced MRI. J Nucl Med. 2009;50:1020–7.
12. Armitage PA, Schwindack C, Bastin ME, Whittle IR. Quantitative assessment of intracranial tumor response to dexamethasone using diffusion, perfusion and permeability magnetic resonance imaging. Magn Reson Imaging. 2007;25:303–10.
13. Murakami R, Sugahara T, Nakamura H, Hirai T, Kitajima M, Hayashida Y, et al. Malignant supratentorial astrocytoma treated with postoperative radiation therapy: prognostic value of pretreatment quantitative diffusion-weighted MR imaging. Radiology. 2007;243:493–9.
14. Higano S, Yun X, Kumabe T, Watanabe M, Mugikura S, Umetsu A, et al. Malignant astrocytic tumors: clinical importance of apparent diffusion coefficient in prediction of grade and prognosis. Radiology. 2006;241:839–46.
15. Hammoud MA, Sawaya R, Shi W, Thall PF, Leeds NE. Prognostic significance of preoperative MRI scans in glioblastoma multiforme. J Neurooncol. 1996;27:65–73.
16. Lacroix M, Abi-Said D, Fourney DR, Gokaslan ZL, Shi W, DeMonte F, et al. A multivariate analysis of 416 patients with glioblastoma multiforme: prognosis, extent of resection, and survival. J Neurosurg. 2001;95:190–8.
17. Al-Agha M, Abushab K, Quffa K, Al-Agha S, Alajerami Y, Tabash M. Efficiency of high and Standard B Value Diffusion-Weighted Magnetic Resonance Imaging in Grading of Gliomas. J Oncol. 2020;2020:6942406.
18. Nguyen TB, Cron GO, Perdrizet K, Bezzina K, Torres CH, Chakraborty S, et al. Comparison of the diagnostic accuracy of DSC- and dynamic contrast-enhanced MRI in the preoperative grading of Astrocytomas. AJNR Am J Neuroradiol. 2017;36:2017–22.
19. Park JE, Kim HS, Park SY, Jung SC, Kim JH, Heo HY. Identification of early response to anti-angiogenic therapy in recurrent glioblastoma: Amide Proton transfer-weighted and perfusion-weighted MRI compared with diffusion-weighted MRI. Radiology. 2020;295:397–406.
20. Pope WB, Kim HJ, Huo J, Alger J, Brown MS, Gjertson D, et al. Recurrent glioblastoma multiforme: ADC histogram analysis predicts response to bevacizumab treatment. Radiology. 2009;252:182–9.
21. Choi SH, Jung SC, Kim KW, Lee JY, Choi Y, Park SH, et al. Perfusion MRI as the predictive/prognostic and pharmacodynamic biomarkers in recurrent malignant glioma treated with bevacizumab: a systematic review and a time-to-event meta-analysis. J Neurooncol. 2016;128:185–94.
22. Buemi F, Guzzardi G, Del Sette B, Sponghini AP, Matheoud R, Soligo E, et al. Apparent diffusion coefficient and tumor volume measurements help stratify progression-free survival of bevacizumab-treated patients with recurrent glioblastoma multiforme. Neuroradiol J. 2019;32:241–9.
23. Patel KS, Everson RG, Yao J, Raymond C, Goldman J, Schlossman J, et al. Diffusion Magnetic Resonance Imaging Phenotypes Predict overall Survival Benefit from Bevacizumab or surgery in recurrent Glioblastoma with large Tumor Burden. Neurosurgery. 2020;87:931–8.
24. Hamstra DA, Rehemtulla A, Ross BD. Diffusion magnetic resonance imaging: a biomarker for treatment response in oncology. J Clin Oncol. 2007;25:4104–9.
25. Schaefer PW, Grant PE, Gonzalez RG. Diffusion-weighted MR imaging of the brain. Radiology. 2000;217:331–45.
26. Yamasaki F, Kurisu K, Satoh K, Arita K, Sugiyama K, Ohtaki M, et al. Apparent diffusion coefficient of human brain tumors at MR imaging. Radiology. 2005;235:985–91.
27. Saksena S, Jain R, Narang J, Scarpace L, Schultz LR, Lehman NL, et al. Predicting survival in glioblastomas using diffusion tensor imaging metrics. J Magn Reson Imaging. 2010;32:788–95.
28. Brasil Caseiras G, Ciccarelli O, Altmann DR, Benton CE, Tozer DJ, Tofts PS, et al. Low-grade gliomas: six-month tumor growth predicts patient outcome better than admission tumor volume, relative cerebral blood volume, and apparent diffusion coefficient. Radiology. 2009;253:505–12.
29. Priola AM, Priola SM, Giraudo MT, Gned D, Fornari A, Ferrero B, et al. Diffusion-weighted magnetic resonance imaging of thymoma: ability of the apparent diffusion coefficient in predicting the World Health Organization (WHO)

classification and the Masaoka-Koga staging system and its prognostic significance on disease-free survival. Eur Radiol. 2016;26:2126–38.

30. Tang J, Liu F, Yuan H, Li X, Tian X, Ji K, et al. Pretreatment apparent diffusion coefficient as a predictor of response to transcatheter arterial chemo-embolization immediately combined with Radiofrequency ablation for treatment of Solitary large Hepatocellular Carcinoma. Cancer Manag Res. 2020;12:10127–38.

31. Giganti F, Orsenigo E, Esposito A, Chiari D, Salerno A, Ambrosi A, et al. Prognostic role of diffusion-weighted MR Imaging for Resectable Gastric Cancer. Radiology. 2015;276:444–52.

32. Lin ZX. Glioma-related edema: new insight into molecular mechanisms and their clinical implications. Chin J Cancer. 2013;32:49–52.

33. Ramnarayan R, Dodd S, Das K, Heidecke V, Rainov NG. Overall survival in patients with malignant glioma may be significantly longer with tumors located in deep grey matter. J Neurol Sci. 2007;260:49–56.

34. Burger PC, Kleihues P. Cytologic composition of the untreated glioblastoma with implications for evaluation of needle biopsies. Cancer. 1989;63:2014–23.

35. Gutman DA, Cooper LA, Hwang SN, Holder CA, Gao J, Aurora TD, et al. MR imaging predictors of molecular profile and survival: multi-institutional study of the TCGA glioblastoma data set. Radiology. 2013;267:560–9.

36. Plate KH, Breier G, Millauer B, Ullrich A, Risau W. Up-regulation of vascular endothelial growth factor and its cognate receptors in a rat glioma model of tumor angiogenesis. Cancer Res. 1993;53:5822–7.

37. Chen WJ, He DS, Tang RX, Ren FH, Chen G. Ki-67 is a valuable prognostic factor in gliomas: evidence from a systematic review and meta-analysis. Asian Pac J Cancer Prev. 2015;16:411–20.

38. Chen JR, Yao Y, Xu HZ, Qin ZY. Isocitrate dehydrogenase (IDH)1/2 mutations as prognostic markers in patients with glioblastomas. Med (Baltim). 2016;95:e2583.

39. Li B, Li H, Zhang L, Ren T, Meng J. Expression analysis of human glioma susceptibility gene and P53 in human glioma and its clinical significance based on bioinformatics. Ann Transl Med. 2023;11:53.

Publisher's note